Materials Science and Engineering B 151 (2008) 238–242

Contents lists available at ScienceDirect

Materials Science and Engineering B

journal homepage: www.elsevier.com/locate/mseb

Short communication

Synthesis of NiCuZn ferrite nanoparticles and microwave absorption characterization

U.R. Lima [a], M.C. Nasar [a], R.S. Nasar [a,*], M.C. Rezende [b], J.H. Araújo [c], J.F. Oliveira [a]

[a] Departamento de Química, UFRN, Cep 59078-970, Natal, RN, Brazil
[b] CTA, IAE, Divisão de Materiais, Cep 12228-904, S.J. Campos, SP, Brazil
[c] Departamento de Física Teórica e Experimental, UFRN, Cep 59078-970, Natal, RN, Brazil

ARTICLE INFO

Article history:
Received 31 January 2008
Received in revised form 13 June 2008
Accepted 29 June 2008

Keywords:
Magnetic materials
Chemical synthesis
X-ray diffraction
Electron microscopy
Magnetic properties

ABSTRACT

This study aimed at the low temperature synthesis of $Ni_xCu_{0.5-x}Zn_{0.5}Fe_2O_4$ ferrite nanoparticles using the citrate precursor method and the reflectivity characterization of Radar absorbing materials. The NiCuZn phase obtained at 350 °C by the Rietveld method showed homogeneous nanoparticle formation. The analysis of particle size and the critical diameter of the domains indicated monodomain formation on nanometric scale. Vibrating sample magnetometry showed that adding copper to NiZn ferrite decreases magnetization saturation and the calcining temperature. Reflectivity measures taken by the wave guide method, obtained absorption radiation of 96.6% for $x = 0.3$ at 12 GHz.

1. Introduction

Recently, the development of ferrite nanomaterials has been studied based on the synthesis of NiZn [1], MnZn [2], MgNi [3] among others [4,5]. In recent years NiZn ferrite which contains various additives, has been synthesized as a compound of radar absorbing material composite. To discover new radiation absorbing materials at high frequencies, Giannakopoulou et al. [6] investigated $NiFe_2O_4$ ferrite prepared by the sol–gel method. Following a mathematical procedure, microwave absorption diagrams were constructed in the 0.1–13 GHz frequency range, including the dependence on the microwave and layer thickness. The permeability spectra widens and microwave absorption improves at 9–10 GHz with an increase in annealing temperature. Yusoff and Abdullah [7] studied the absorption characteristics of undoped and doped samples (1 wt% CuO and MgO) of $(Li_{0.5}Fe_{0.5})_{0.7}Zn_{0.3}Fe_2O_4$ ferrite in the 0.3–13.51 GHz frequency range. The addition of CuO and MgO has been found to increase the reflectivity and transmittivity of pure ferrite. Jian et al. [8] studied the microwave absorbing properties of $(Ni_{1-x-y}Co_xZn_y)Fe_2O_4$ ferrite within the 0.5–14 GHz frequency range. They observed the absorbing frequency band (AFB) from 8.64 to 11.2 GHz. Cheng et al. [9] synthesized nanoparticles of silver doped $(Ni_{0.5}Zn_{0.5}Fe_2O_4)$ ferrite using the hydrothermal method. An analysis from 2 to 15 GHz shows −25 dB of radiation absorption at 9 GHz. The real contribution of copper added to NiZn ferrite to radiation absorption in the microwave range was not investigated. NiCuZn ferrite has been used in the manufacturing of multiplayer chip inductors in high frequency regions [10] showing potential for use at ultra high frequencies. The purpose of our study was to synthesize nanometric $Ni_xCu_{0.5-x}Zn_{0.5}Fe_2O_4$, where Nickel varied from $0.2 \leq x \leq 0.4$ at low temperatures and study the influence of copper on magnetic characteristics and absorption radiation in a range of 8–12 GHz.

2. Experimental procedure

2.1. Synthesis

The nanometric ferrite powders of various $Ni_xCu_{0.5-x}Zn_{0.5}Fe_2O_4$ compositions ($0.2 \leq x \leq 0.4$) were prepared using ferric nitrate, zinc nitrate, nickel nitrate and copper nitrate with high chemical purity. Various nitrate solutions were prepared with the addition of 100 ml of distilled water and homogenized for 1 h. Citric acid at a 3:1 molar ratio was mixed, forming a colored solution of citrates homogenized for 2 h under agitation. A stoichiometric mixture of citrate solutions according to the above formula were prepared under agitation for 3 h at a temperature of 70 °C. The citrate solutions were decomposed at 350 °C in an oven with ambient atmosphere for 3 h. The different compositions were calcined from 500 to 1200 °C using an argon atmosphere for 3 h.

* Corresponding author. Tel.: +55 32153828; fax: +55 32119224.
E-mail address: nasar@terra.com.br (R.S. Nasar).

0921-5107/$ – see front matter © 2008 Elsevier B.V. All rights reserved.
doi:10.1016/j.mseb.2008.06.032

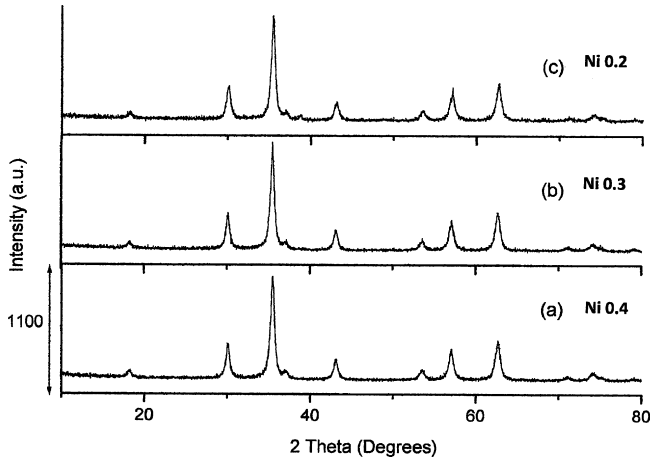

Fig. 1. X-ray diffraction pattern of powder calcined at 350 °C at ambient temperature.

2.2. Characterization

The X-ray diffraction pattern was performed using a Shimadzu XRD 6000 with Cu Kα radiation of 1.5418 Å, work tension of 30 kV and current of 20 mA. Rietveld refinement was used with a MAUD program version-2.044. Scanning electron microscopy (SEM) of the calcined powder was analyzed using a Philips XL 30 ESEM with acceleration voltage of 20 kV. The magnetic measures were taken with an X752 direction coupler (Hewlett Packard), an 83752A synthetized seeper (Agilent) and a 70000 spectrum analyzer (Hewlett Packard).

2.2.1. Wave guide measures

Wave guide measures were taken in a frequency range between 8 and 12 GHz. The directional coupler had high mechanical precision, consisting of two connected wave guides. The directional coupler was projected in such a way that the electromagnetic wave covered it as follows: the microwave source was connected to terminal A, where it covered the wave guide to reach terminal B. The electromagnetic wave that covers the direction from A to B, in it reaches terminal C. The sample in this study, which was located in terminal B, measured 23 mm × 11 mm and used a support developed with precise dimensions of the directional coupler.

3. Results and discussion

Fig. 1 shows the X-ray diffraction pattern of powder calcined at 350 °C/3.5 h in ambient atmosphere for Nickel concentration varying from $0.2 \leq x \leq 0.4$. Only one phase was formed for all compositions; it showed a peak of NiCuZn ferrite at low temperatures. Wang et al. [4] synthesized NiCuZn ferrite using the citrate precursor method, obtaining nanoparticles at 700 °C. Table 1 shows the particle size obtained by the Rietveld method. Nanometric particle formation was observed at 350 °C/3.5 h.

To avoid hematite precipitation, the powder was calcined in an argon atmosphere at 1000 °C/3 h and 1100 °C/3 h. The X-ray diffraction pattern of the powder (Fig. 2) shows NiCuZn ferrite formation

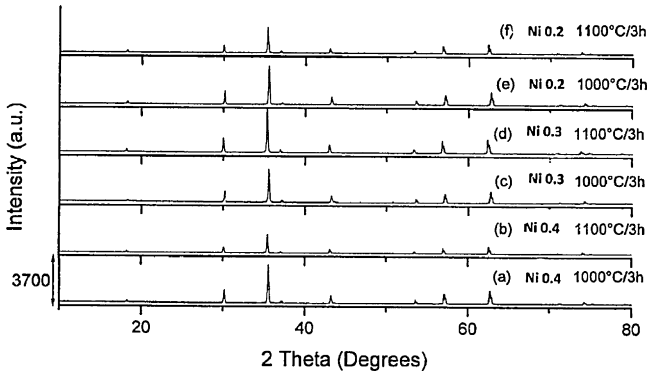

Fig. 2. X-ray diffraction pattern of powder calcined at 1000 °C and 1100 °C/3 h in an argon atmosphere.

without hematite phase formation. Independent of the nickel concentration the high defined peaks of the NiCuZn phase showed homogeneous crystallinity. The particle size (Table 2) increased from 21 nm at 350 °C to above 435 nm at 1000 °C. The decrease of nickel substitutions into the lattice inhibits grain growth during calcinations. Low and Sale [11] synthesized NiCuZn ferrite, whose particle size increased during calcinations. According to the Rietveld refinement the calculated stoichiometries of compounds were:

- $x = 0.2(Zn_{0.50}Cu_{0.07}Fe_{0.54})^{Tetr.}[Ni_{0.10}Cu_{0.115}Fe_{0.73}]^{Oct.}{}_2O_4$;
- $x = 0.3(Zn_{0.50}Cu_{0.014}Fe_{0.50})^{Tetr.}[Ni_{0.15}Cu_{0.093}Fe_{0.75}]^{Oct}{}_2O_4$;
- $x = 0.4(Zn_{0.50}Cu_{0.02}Fe_{0.48})^{Tetr.}[Ni_{0.20}Cu_{0.04}Fe_{0.76}]^{Oct.}{}_2O_4$.

Scanning electron microscopy (SEM) of powder calcined at 1000 °C/3 h (Fig. 3a, c and e) and 1100 °C/3 h (Fig. 3b, d and f), shows an increase in particle size from a nickel concentration of $x = 0.2$–0.4. The average crystal size analyzed by SEM is close to that obtained by the Rietveld method. It was not observed the copper oxide phase by X-ray diffraction in consequence of the superimposition of all the peaks in those peaks of the ferrimagnetic phase. Fig. 3c–f shows small particles of copper oxide phase around the boundaries of particles of ferrimagnetic phase.

An evaluation of the critical diameter (d_{cr}) of the particle was done, considering a spherical particle model [12]. The d_{cr} can be calculated using the equation:

$$d_{cr} = \frac{9\varepsilon_P}{2\pi M_S} \quad (1)$$

where ε_P is the surface energy of the domain wall and M_S is the spontaneous magnetization. The energy surface, ε_P can be expressed as a function of k_B, the Boltzmann constant, T_C (Curie temperature), K_1, the magneto crystalline anisotropy constant, and a, the lattice parameter, as follows:

$$\varepsilon_P = \left(\frac{2k_B T_C K_1}{a}\right)^{1/2} \quad (2)$$

Table 1
Lattice parameters and crystal size of NiCuZn ferrite

Composition (x)	Temperature (°C)	Lattice parameters (Å)	Crystal size (nm)
0.2	350	8.3819	21.63
0.3	350	8.3882	21.01
0.4	350	8.3858	21.25

Table 2
Lattice parameters and crystal size of NiCuZn ferrite above of 350 °C

Composition (x)	Temperature (°C)	Lattice parameters (Å)	Crystal size (nm)
0.2	500	8.3965	21.02
0.2	1000	8.3689	461.67
0.3	500	8.4037	62.03
0.3	1000	8.3689	435.62
0.4	500	8.3968	57.91
0.4	1000	8.3666	578.91

In Eq. (2) we have replaced $K_1 = 1.5 \times 10^4$ erg/cm^3, $T_C = 425$ K, $k_B = 1.38 \times 10^{-16}$ erg/K, and the calculated lattice constant $a = 8.39 \times 10^{-8}$ cm by $x = 0.3$ resulting in $\varepsilon_P = 0.1448$ erg/cm^2. The critical diameter of the powder particle calcined at 1000 °C/3 h was 13.05 nm ($x = 0.3$) and the particle size was 435.62 nm ($x = 0.3$). This could indicate that multidomains were formed considering the growth of the particle. The domain structure is formed at the nanometric level. We used a simplified model, which does not take into account the shape of the particles, the interactions between the particles and the surface effects.

Fig. 4 shows an increase in calcining temperature decreases magnetization saturation (M_S) with copper additions into the NiZn lattice. When copper ion substitution compensates the energy interaction by nickel ions substitutions in [B] positions, the magnetization decreases with an increase in copper ions. NiZn ferrite has 12 Fe ions ($3d^6 4s^2$) in octahedral positions and 4 Ni ions ($3d^8 4s^2$) in tetrahedral positions. Inversely positioned has 4 Fe ions in tetrahedral positions and 4 Zn ions ($3d^{10} 4s^2$) in octahedral positions. The copper ($3d^{10} 4s^1$) partially substitutes 4 tetrahedral positions of Ni and 4 inverse octahedral positions of Zn. Thus, 4 tetrahedral Fe ions positions are annulled with 4 of octahedral Fe ions positions. The decrease of nickel concentration increased the level of occupa-

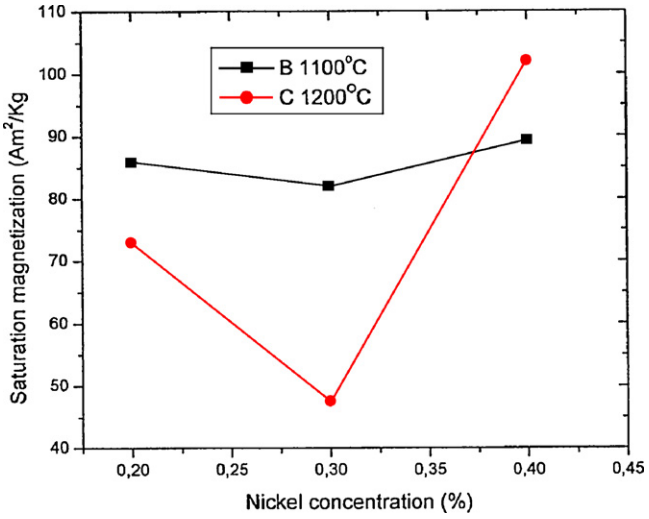

Fig. 4. Saturation magnetization (M_S) of powder calcined at 1000 °C and 1100 °C/3 h.

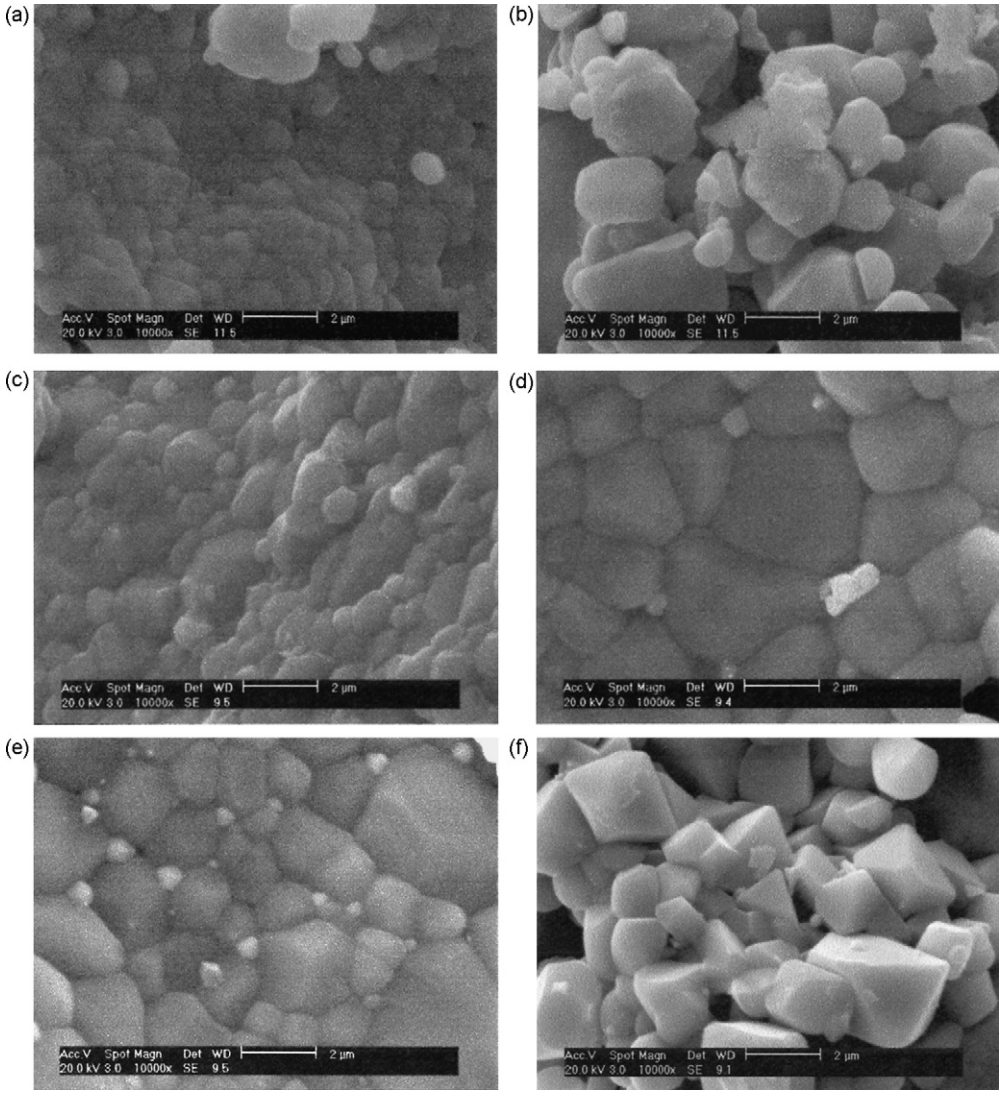

Fig. 3. Scanning electron microscopy (SEM) of powder calcined at 1000 °C/3 h and 1100 °C/3 h.

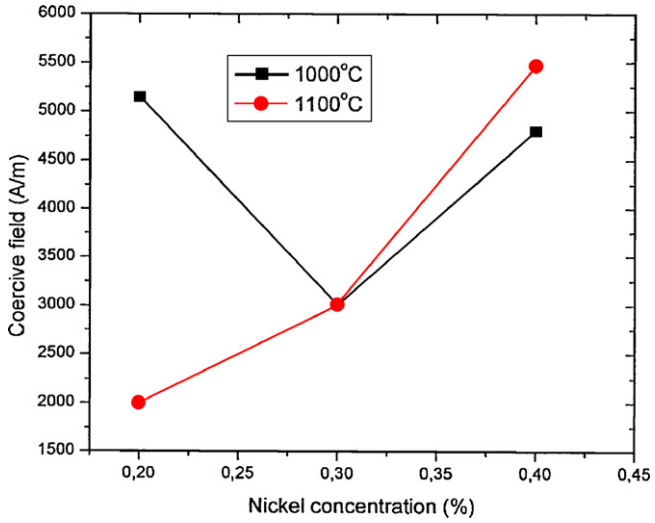

Fig. 5. Coercive field of powder calcined at 1000 °C and 1100 °C/3 h.

tion of copper in inverse octahedral positions. As a consequence a decrease of total magnetization effect occurs.

Complementary data show that excess copper in the NiZn lattice caused CuO formation and decreased the magnetic characteristics (Fig. 4) of the powder. According to Shrotri et al. [13] the decrease of nickel in NiZn ferrite inhibits particle growth and decreases the saturation magnetization of the powder. Copper increment substituted Zn and Ni positions and caused oxygen vacancies formation. These defects led to tension into relief in the domain walls limit and facilitate the expansion when is submitted to magnetic fields. The increase of copper concentration caused partial substitution in tetrahedral positions of Ni and octahedral positions of Zn decreasing the total magnetic effect.

The coercive field (Fig. 5) exhibit the same behavior as that displayed by the particle size (Table 2), showing coercive field decrease, indicating that the magnetic characteristics are those of soft materials, with low magnetization to reverse spin direction.

Fig. 6 shows a decrease of coercive field with an increase of crystal size indicating that multidomains are formed. For $x = 0.3$ the curve decay near to 100 nm. Multidomains in small crystals difficult domain expansion in magnetic fields. Analysis of $x = 0.4$ composition show a decrease of coercive field after 30 nm indicating that the domains expanded until 700 nm (0.7 μm) with possibility to obtain high magnetization. The $x = 0.2$ concentration form multidomains after 100 nm with rapid domains increase until 500 nm (0.5 μm).

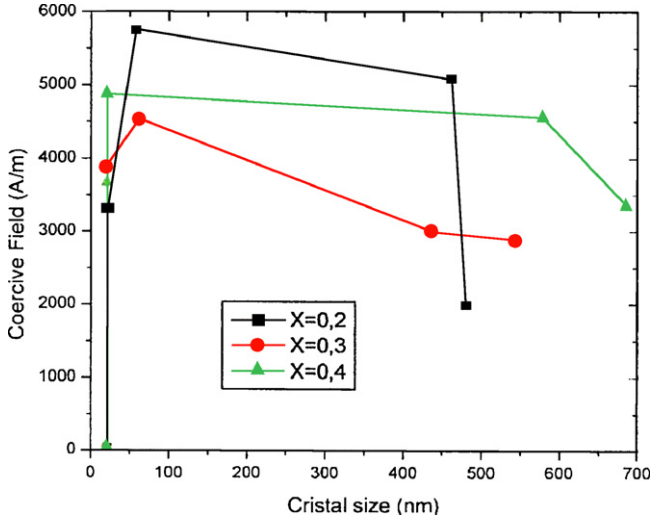

Fig. 6. Coercive field versus crystal size for different concentrations.

Table 3
Average attenuation and absorption radiation of NiCuZn ferrite

Composition (x)	Average attenuation (dB)	Absorption radiation (%)
0.2	1	21
0.3	<1	<21
0.4	<1	<21

Reflectivity measures of composite epoxy-ferrite with the powder calcined at 1000 °C (Table 3) shows radiation absorption close to 21% for a nickel concentration of $x = 0.3$. Below 21% of radiation absorption was observed for $x = 0.4$ and 0.2. The powder calcined at 1100 °C shows attenuation of 90% for $x = 0.2$ (Fig. 7) and 96.6% for $x = 0.4$ (Fig. 8) at 12 GHz. Dias et al. [14] studying RAM based on polyurethane and NiZn ferrite achieved attenuation of 70% at 12 GHz. Different from copper, the addition of silver decreases band frequency absorption at 9 GHz (−25 dB). According to the results, the decrease of Ni and increment of copper caused an optimization of absorption radiation at high frequencies. Remnant magnetization, M_R of $x = 0.4$ composition was 18 A m^2/kg for the material sintered at 1100 °C/3 h. The powder sintered at 1000 °C/3 h was

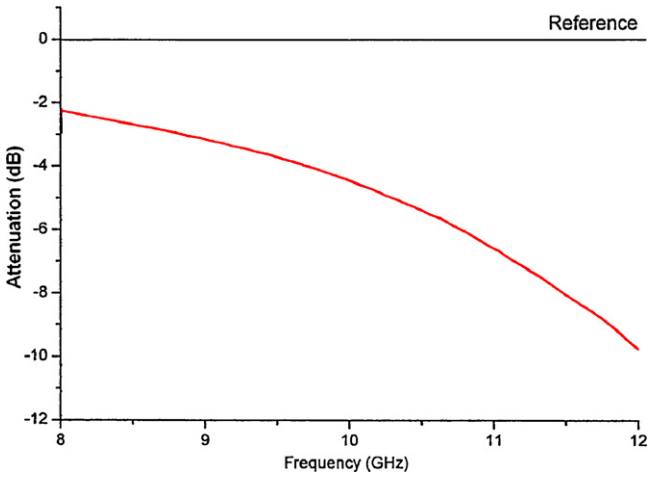

Fig. 7. Reflectivity of powder for $x = 0.4$ calcined at 1100 °C/3 h.

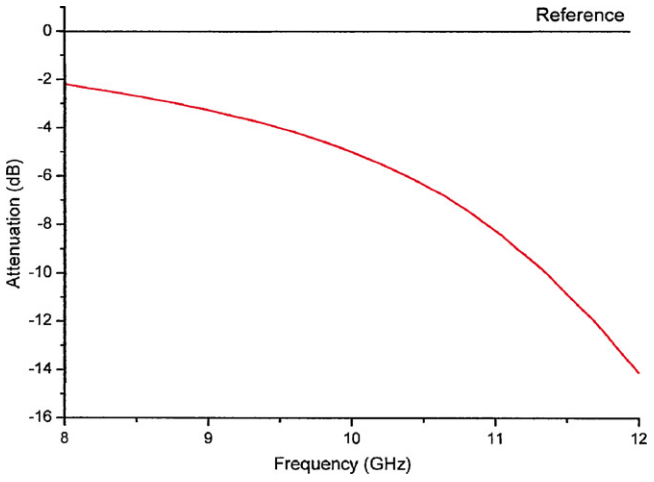

Fig. 8. Reflectivity of powder for $x = 0.3$ calcined at 1100 °C/3 h.

7.2 A m^2/kg and in $x = 0.2$ sintered at 1100 °C/3 h was 6.9 A m^2/kg. The high M_R indicated that macro domains absorb more electromagnetic radiation and obtain high reflectivity. Thus, the effect into the domains diminished M_R during absorption and returned to high magnetization after energy dissipation. The degradation process of material occurs after several absorptions with a decrease of magnetization due to volume reduction of domains.

It is reported [12] that at a temperature slightly above 1000 °C, the CuO phase decomposes to Cu_2O, and due to the formation of Cu^{1+} and Cu^{2+} conduction increases, thereby decreasing its resistivity value. The increased conduction led to much higher heat dissipation and altered wave absorption characteristics.

4. Conclusions

The synthesis performed using the citrate precursor method led to the formation of nanoparticles that are applied to Radar absorbing materials. The electromagnetic measures indicated a powder with high magnetization saturation and low coercive field, characterizing a soft ferrite material. Reflectivity measures obtained were around 96.6% of radiation absorption in the powder with copper concentration of $x = 0.2$ at 12 GHz. These results indicate that copper additions resulted in very promising material that can be used in Radar absorption material.

References

[1] W.-C. Hsu, S.C. Chen, P.C. Kuo, C.T. Lie, W.S. Tsai, Mater. Sci. Eng. B111 (2004) 142–149.
[2] C. Rath, K.K. Sahu, S. Anand, S.K. Date, N.C. Mishra, R.P. Das, J. Magn. Magn. Mater. 279 (2004) 103–110.
[3] M. Sinha, H. Dutta, S.K. Pradhan, Physica E 28 (2005) 43–49.
[4] X. Wang, W. Qu, L. Li, Z. Gui, Ceram. Int. 30 (2004) 1615–1618.
[5] R.H. Kodama, J. Magn. Magn. Mater. 200 (1999) 359.
[6] T. Giannakopoulou, L. Kompotiatis, A. Kontogeorgakos, G. Kordas, J. Magn. Magn. Mater. 246 (2002) 360–365.
[7] A.N. Yusoff, M.H. Abdullah, J. Magn. Magn. Mater. 269 (2004) 271–280.
[8] L.X. Jian, H. Mangui, L. Chen, K. Renxiong, D. Longjiang, J. Magn. Magn. Mater. 314 (2007) 37–42.
[9] H.P. Cheng, W.W. Hong, W.K. Shih, Z.S. Ming, M.W. Yu, Y.C. San, J. Magn. Magn. Mater. 284 (2004) 113–119.
[10] Y.P. Fu, K.Y. Pan, C.H. Lin, Mater. Lett. 57 (2002) 291–296.
[11] K.O. Low, F.R. Sale, J. Magn. Magn. Mater. 246 (2002) 30–35.
[12] J. Smit, H.P.J. Wijin, Les Ferrites, Bibl. Tech. Philips, Paris, 1961.
[13] J.J. Shrotri, S.D. Kulkarni, C.E. Deshpande, A. Mitra, S.R. Sainkar, P.S. Anil kumar, S.K. Date, Mater. Chem. Phys. 59 (1999) 1–5.
[14] J.C. Dias, I.M. Martin, E.L. Nohara, M.C. Rezende, Ver. Fis. Appl. Instrum. 18 (2005) 24–33.